Forest Vegetation of the Colombian Orinoquia: Characterization and Spatial Distribution Across Environmental Gradients

Larry Niño , Orlando Rangel , Diego Giraldo-Cañas , Daniel Sánchez-Mata , Vladimir Minorta-Cely *

Posted Date: 22 April 2026

doi: 10.20944/preprints202604.1593.v1

Keywords: neotropical savannas; phytosociology; forests mapping; random forest; multi-sensor remote sensing; environmental gradients; Colombian Orinoquia

 doi:10.20944/preprints202604.1593.v1

Article

Forest Vegetation of the Colombian Orinoquia: Characterization and Spatial Distribution Across Environmental Gradients

Larry Niño [1], Orlando Rangel [1], Diego Giraldo-Cañas [1], Daniel Sánchez-Mata [2,3] and Vladimir Minorta-Cely [4,*]

[1] Natural Science Institute, National University of Colombia, Bogotá D.C., 111321, Colombia
[2] Botany Unit, Faculty of Pharmacy, Complutense University of Madrid, 28040, Spain
[3] Department of Organismic and Evolutionary Biology (OEB), Harvard University Herbaria, Harvard University, Cambridge, MA 02138, USA
[4] Biology Program and Natural Sciences Services, Central University, Bogotá D.C. 111711, Colombia
* Correspondence: vminortac@ucentral.edu.co

Abstract

Vegetation spatial heterogeneity is fundamental to biodiversity management and ecosystem service provision, yet detailed phytosociological mapping of forest vegetation remains largely unresolved in the Colombian Orinoquia. This study characterized the geographic distribution of forest vegetation through the integration of 178 field surveys, environmental complex variables defined by geomorphological and bioclimatic gradients, and multi-sensor satellite imagery combining Landsat-8 optical bands and Sentinel-1 dual-polarization data, processed within a Random Forest classification framework in Google Earth Engine. Classifications achieved overall accuracies between 0.910 and 0.975 and Kappa coefficients above 0.93, identifying 24 phytosociological alliances or geobotanical formations distributed across approximately 7,565,696 ha, representing 34.63% of the region. Forest cover ranges from 10.95% in the Floodplain to 55.22% in La Macarena, with the High Plain concentrating the greatest formation diversity. The spatial organization of forest vegetation is primarily governed by the geomorphological gradient — fluvial, denudational, and structural — and limiting bioclimatic factors, together with their associated edaphic-hydrological regimes, with anthropic transformation driven by cattle ranching and agricultural expansion constituting the principal threat to forest cover. These results advance beyond existing land cover surrogates, providing an empirically validated cartographic framework for biodiversity assessment, habitat modeling, and natural capital management in the Colombian Orinoquia.

Keywords: neotropical savannas; phytosociology; forests mapping; random forest; multi-sensor remote sensing; environmental gradients; Colombian Orinoquia

1. Introduction

The spatial heterogeneity of vegetation, understood as the set of plants that establish spontaneously in a particular area [1], is fundamental to land use planning and biodiversity management, given that primary productivity supports most of the ecological functions upon which the abundance and distribution of other life forms depend [2]. As a fundamental structural component of terrestrial ecosystems, vegetation regulates fluxes in biogeochemical cycles [3], influences climatic processes, the albedo effect, and the exchange of water and heat [4]; its patterns respond to environmental factors such as climate and topography, the physiological responses of the plant populations present, and the structural and functional characteristics of vegetation types [5]. In the Orinoquia, the geographic distribution, structure, and floristic composition of vegetation are influenced by environmental heterogeneity, particularly by physiographic and climatic variations [6–

 doi:10.20944/preprints202604.1593.v1

10], which is why understanding its diversity and distribution across different scales is essential for the provision of ecosystem services and the management of natural capital [11,12].

Environmental complexes, defined as the sum of interrelated physical factors that shape landscapes along gradients [5], influence biodiversity through factors that limit the eco-physiology of organisms, disturbances that affect environmental conditions, and resources assimilable by organisms [13,14]. While bioclimatic gradients are direct determinants of species physiology, topographic gradients show high correlation with the distribution of biota [15–18]; mechanistic models integrating spectral data with climatic factors have demonstrated strong performance in the spatial characterization of vegetation [19]. Although the temporal and spatial resolution of climatic data had previously constituted a limiting factor in the characterization of biodiversity at regional scales, modeling studies have overcome these challenges through static and probabilistic correlations between occurrence points and climatic means over extended periods [20,21], with bioclimatic indices serving as valuable tools for establishing thresholds associated with climatic periods that impact vegetation through water and thermal stress [22,23]. Within this framework, geomorphological factors, together with mesoclimatic patterns, constitute the main predictor variables of the geographic distribution of current vegetation along diverse environmental gradients [24–30].

Characterizing these gradients and their influence on vegetation at regional scales requires spatially continuous data that fieldwork alone cannot provide. Optical remote sensors allow territories to be described by overcoming the spatial, temporal, and economic limitations of fieldwork [31]; their use in the elaboration of vegetation maps is based on the reflectivity and emissivity of plants captured from space, which allows the differentiation of elements on the Earth's surface [32] and the identification of functional characteristics of dominant plants as predictors of physiological adaptations to environmental conditions [33–35], enabling the mapping of floristic assemblages with unique taxonomic compositions in heterogeneous landscapes [36,37]. Complementarily, Synthetic Aperture Radar (SAR) imagery provides information on the physical and dielectric properties of the natural environment [38,39], and its integration with optical imagery allows the enhancement of geobotanical landscape features and overcomes limitations in the statistical differentiation based on spectral variability in digital classifications [40–43]. Given the challenges posed by the processing of large volumes of satellite data at extensive scales, platforms such as Google Earth Engine (GEE) offer a solution by providing automated parallel computing with access to petabytes of planetary-scale remote sensing information, overcoming the computational capacity and storage limitations of traditional cartographic techniques [44–48].

The characterization of the Earth's surface using remote sensors has evolved from the visual comparison of images toward automated digital classification methods, grouped into unsupervised categories, which cluster pixels by minimum distance, and supervised categories, which assign classes based on training areas with a high degree of certainty [49–51]. In the Colombian Orinoquia, although thematic cartography has been predominantly based on visual interpretations, parametric models such as maximum likelihood have been implemented [52–54]; however, Machine Learning techniques, in particular Random Forest, have gained special attention for their high accuracy, rapid processing, and non-parametric nature, which facilitates the classification of data that do not follow a normal distribution and of multidimensional images from diverse sources [55–58].

In Colombia, conservation is currently managed through biodiversity surrogates such as land cover and land use maps. Although useful, these can be problematic when their correspondence with the actual distribution of biodiversity is low [59,60]. Detailed thematic cartography proves more effective in addressing environmental conflicts and improving biodiversity management [36,61]. Multi-sensor applications facilitate the development of new technological approaches and overcome inherent technical limitations [48]. The integration of field data and satellite imagery allows the gap between remote sensing and ecology to be bridged, promoting effective methods for assessing biodiversity at large scales in a continuous and detailed manner [34,62,63]. This study aims to advance the understanding of vegetation diversity and distribution in the Colombian Orinoquia by characterizing the geographic distribution of current vegetation through the integration of

 doi:10.20944/preprints202604.1593.v1

phytosociological field data, the environmental complex defined by geomorphological and bioclimatic gradients, and multi-sensor satellite imagery combining Landsat-8 optical bands and Sentinel-1 dual-polarization data. This approach seeks to bridge the gap between remote sensing and ecology, contributing to more effective biodiversity assessment and natural capital management at regional scales.

2. Results

The Random Forest models classified stacked images into discrete units according to the previously delineated phytosociological alliances or formations. The optimal parameterization of decision trees ranged from 60 (Foothills) to 110 (High Plain), with overall accuracies of 0.975 and 0.910, respectively. This indicates a 91–97% agreement between classified pixels and reference categories. Confusion matrices allowed accuracy to be evaluated through the concordance of main diagonals, error distribution, and non-random pixel assignments. Maximum omission and commission errors were 17% and 13%, respectively, both associated with the High Plain. The Kappa coefficient, which measures the difference between automatic and random classifications [64,65], reached minimum values of 0.93, reflecting a low probability of random classification. This digital approach contributes consistency and reproducibility, avoiding the biases inherent in visual classifications [61,66]. The robustness of these classifications, supported by overall accuracies and Kappa coefficients, provides a reliable basis for the spatial interpretation of vegetation distribution at the regional scale. The following sections describe the geographic distribution of the 24 phytosociological alliances or geobotanical formations identified across the four subregions of the Colombian Orinoquia.

Analyses of the current vegetation distribution in the Colombian Orinoquia reveal that 73.74% of its territory retains a natural vegetation cover. Of this area, 34.63% is occupied by 24 forest formations. The data presented in Table 1 correspond to 24 phytosociological alliances or geobotanical formations distributed across the Colombian Orinoquia, with a total area of approximately 7,565,696 ha. The alliance with the greatest representation is *Attaleo maripae – Iryantherion laevis* with 3,478,544 ha (14.89%), which distinguishes it markedly from the remaining units and suggests its dominant role in shaping the forest landscape of the region. It is followed in extent by *Spondiado mombinis – Viticion orinocensis* (1.82%), *Chamaedoreo pinnatifrondis – Sloaneion brevispinae* (1.45%), and *Bowdichio virgilioidis – Curatellion americanae* (2.32%), while most of the remaining alliances occupy between 0.62% and 1.33% of the total area. In contrast, the units with the least representation are *Phenakospermo guyannensis – Attaleetion maripae* (0.03%), *Protio heptaphylli – Jacarandion obtusifoliae* (0.04%), and *Coccolobo caracasanae – Tapiriretion guianensis* (0.09%), whose limited extent may indicate particular disturbance, overexploitation, or environmental conditions that restrict their distribution. Overall, the distribution of alliances reflects a marked asymmetry in territorial occupation, where a single unit concentrates nearly 15% of the total surface area, while the majority of formations are distributed in comparatively smaller and relatively equitable extents — a pattern that highlights the physiognomic and floristic heterogeneity characteristic of the forests of the Colombian Orinoquia.

 doi:10.20944/preprints202604.1593.v1

Table 1. Area of the Orinoquia currently covered by natural forests.

Phytosociological Alliance/Geobotanical formation	Area (ha)	Area (%)
Bowdichio virgilioidis - Curatellion americanae	541,913.67	2.32
Gongylolepis martiana - Bonnetia sessilis	25,732.04	0.11
Alchorneo triplinerviae - Maurition flexuosae	237,443.02	1.02
Attaleo maripae - Iryantherion laevis	3,478,544.43	14.89
Batocarpo orinocensis - Senefelderion verticillatae	101,250.31	0.43
Brosimo lactescentis - Euterpion precatoriae	113,448.85	0.49
Chamaedoreo pinnatifrondis - Sloaneion brevispinae	337,508.51	1.45
Coccolobo caracasanae - Tapiriretion guianensis	21,479.33	0.09
Copaifero pubiflorae - Protion guianensis	144,128.58	0.62
Duguetio quitarensis - Amphirrhocion longifoliae	310,583.23	1.33
Enterolobio schomburgki - Terminalion amazoniae	195,241.85	0.84
Lueheo seemani - Pseudolmedion laevigatae	31,621.22	0.14
Guatterio hirsutae - Oenocarpion minoris	227,847.09	0.98
Micranda spruceana and species of Eschweilera	284,104.91	1.22
Ocoteo cernuae - Viticion orinocensis	208,635.48	0.89
Oenocarpo minoris - Attaleion maripae	243,766.50	1.04
Oenocarpus bataua - Protium rhoifolium	172,849.21	0.74
Phenakospermo guyannensis - Attaleetion maripae	7,518.72	0.03
Protio aracouchini - Oenocarpion batauae	45,944.29	0.20
Protio guianensis - Caraipion llanori	229,229.48	0.98
Protio heptaphylli - Jacarandion obtusifoliae	9,484.38	0.04
Siparuno guianensis - Maurition flexuosae	221,191.47	0.95
Spondiado mombinis - Viticion orinocensis	424,117.03	1.82
Syagro orinocensis - Virolion elongatae	160,110.02	0.69

2.1. Foothills Forests

Natural forest vegetation represents only 12.51% of its territory (Figure 1), evidencing that 86.06% of natural covers have been transformed, primarily by the expansion of cattle ranching and monocultures such as oil palm and rice [67]. Six forest vegetation formations are recognized in this subregion, with a predominance of *Brosimo lactescentis – Euterpion precatoriae*, located in the fluvial environments of the main rivers, followed by *Ocoteo cernuae – Viticion orinocensis*, distributed toward the higher-elevation margin of the Foothills bordering the Eastern Cordillera, frequently occurring in structural geomorphological environments [57]. Natural forest remnants persist on steep terrain whose slope and edaphic characteristics are not conducive to agricultural activities; however, forests that have lost their original structure due to human intervention are maintained on these same terrains under continuous selective logging and, in more advanced stages of degradation, consist primarily of shrublands located on low-gradient terrain within the fluvial environment, where selective felling gives way to generalized clearing as a precursor to the establishment of agricultural activities [68].

 doi:10.20944/preprints202604.1593.v1

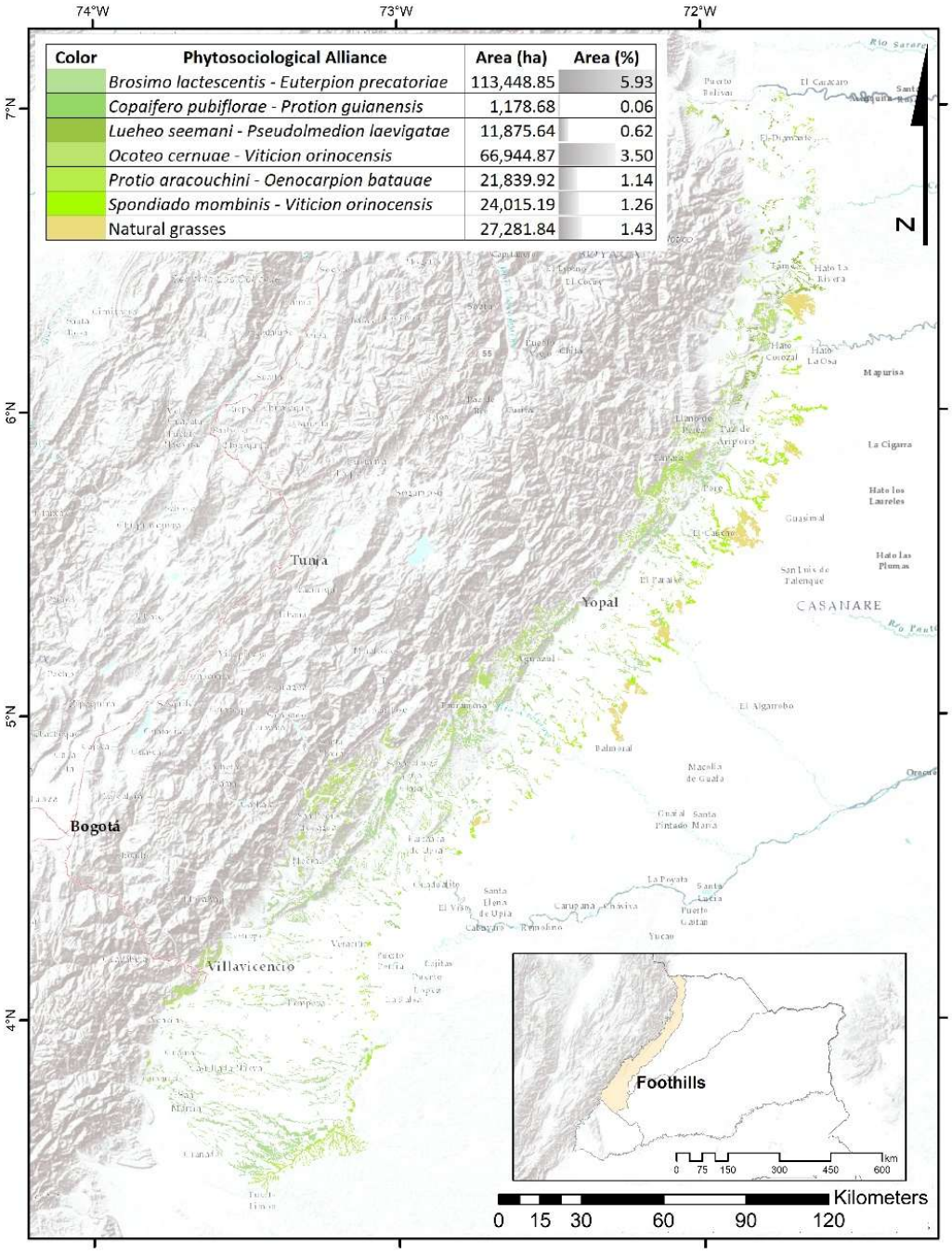

Figure 1. Spatial distribution and area of forests phytosociological alliances in the Foothills of the Colombian Orinoquia.

2.2. La Macarena Forests

Natural forest vegetation represents 55.22% of its territory; however, 39.38% of natural covers have been transformed, primarily by the expansion of pastures for extensive cattle ranching, the enlargement of the agricultural frontier, uncontrolled burning, and human settlements — processes that advance preferentially through non-flooded forest areas with well-drained, less acidic soils [69–71]. Eight forest vegetation formations were identified in this subregion, with a predominance of *Chamaedoreo pinnatifrondis – Sloaneion brevispinae*, rooted predominantly in the structural and

 doi:10.20944/preprints202604.1593.v1

denudational environments of the massif and the cordilleran foothills, followed by *Micranda spruceana* and species of *Eschweilera*, distributed over denudational hills north of the Guayabero River, and *Oenocarpus bataua – Protium rhoifolium*, located likewise over denudational hills between the Central River and the mouth of the Ariari River. Complementarily, *Syagro orinocensis – Virolion elongatae* is distributed across fluvial and denudational environments on the western slope of the massif and on terraces south of the Guayabero River, while the low forest of *Bowdichio virgilioidis – Curatellion americanae* occupies the low-gradient structural environment, and the shrubland of *Gongylolepis martiana – Bonnetia sessilis* is restricted to structural hillsides and slopes of the massif with frequent rocky outcrops (Figure 2).

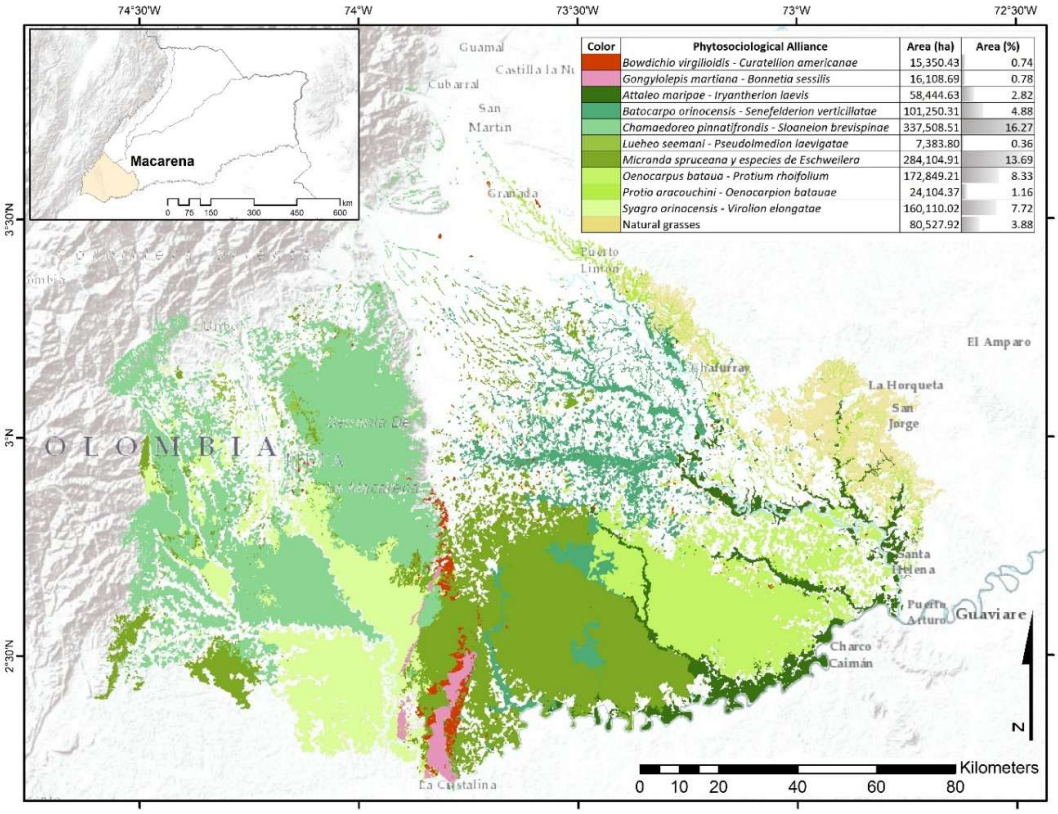

Figure 2. Spatial distribution and area of forests phytosociological alliances in La Macarena of the Colombian Orinoquia.

2.3. Floodplain Forests

Natural forest vegetation represents only 10.95% of its territory, while human activities have transformed 33.86% of natural covers, with agricultural and livestock modifications located primarily in lowlands, floodplain banks, and river levees of the Lipa, Ele, and Cravo Norte rivers and their tributaries, where acidity levels and aluminum concentrations are lower than on the terraces [72]. Eight forest formations were identified in this subregion, all associated with floodplains, with a predominance of *Spondiado mombinis – Viticion orinocensis*, located primarily on the floodplains associated with the tributaries of the Meta River in the central and northern sections of the eastern flank, followed by *Copaifero pubiflorae – Protion guianensis* and *Ocoteo cernuae – Viticion orinocensis*, distributed over floodplains associated with denudational plains located toward the northwest and over the tributaries of the Meta River to the south, respectively. The formations with lesser spatial representation include *Vitici orinocencis – Mabeetion trianae* on the floodplains of the Arauca River tributaries to the north; *Lueheo seemani – Pseudolmedion laevigatae* on the floodplains of the Lipa and

 doi:10.20944/preprints202604.1593.v1

Casanare rivers adjacent to denudational plains toward the northwest; *Protio heptaphylli – Jacarandion obtusifoliae* on the floodplains of the Cinaruco River associated with denudational and aeolian environments; *Phenakospermo guyannensis – Attaleetion maripae* in the northeastern extreme where the aeolian environment prevails; and *Coccolobo caracasanae – Tapiriretion guianensis* on plains adjacent to loess sheets near the Meta River (Figure 3).

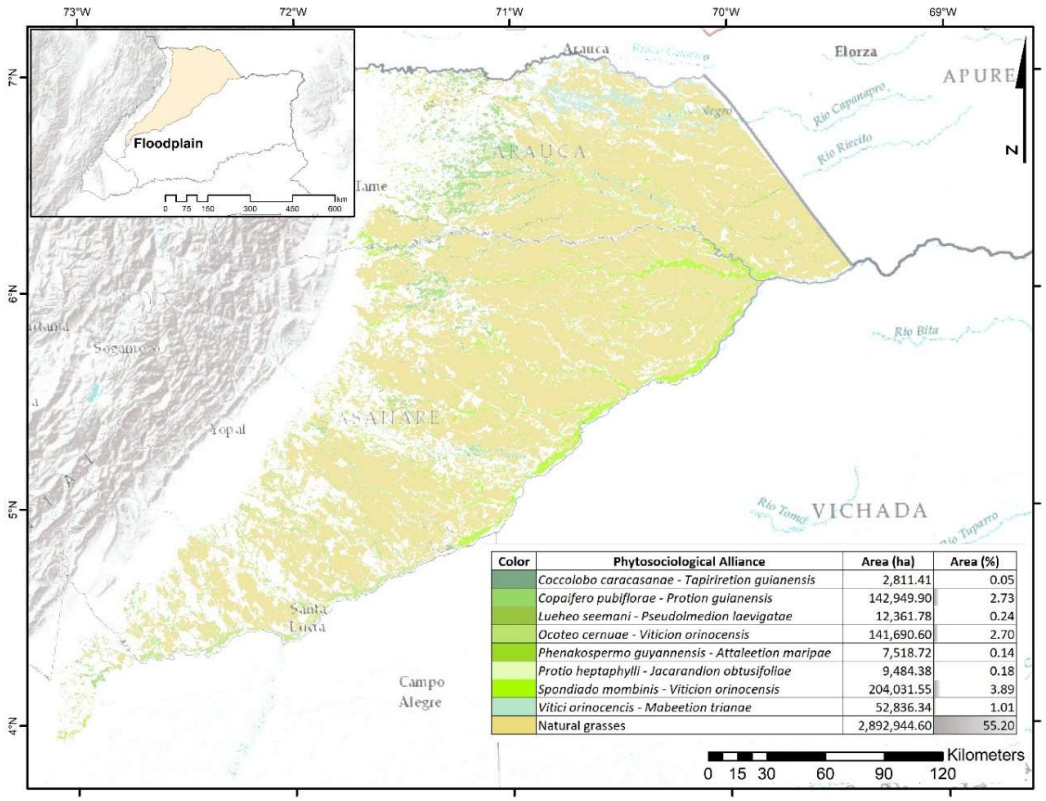

Figure 3. Spatial distribution and area of forests phytosociological alliances in the Floodplain of the Colombian Orinoquia.

2.4. High Plain Forests

Natural forest vegetation represents 39.30% of its territory (Figure 4), making this the subregion with the greatest diversity of forest formations, totaling 11, where anthropic activity has transformed 13.55% of natural covers, particularly within the fluvial environment where chemical reduction improves soil fertility properties, favoring the establishment of agricultural and livestock activities in originally forested areas [68]. *Attaleo maripae – Iryantherion laevis* predominates extensively, its distribution encompassing the denudational environment bounded to the east by the Siare River, to the west by the Orinoco River, to the north by the highly dissected hills associated with the Vichada River, and to the south by the fluvial environment of the Guaviare River. It is followed in spatial representation by *Duguetio quitarensis – Amphirrhocion longifoliae*, associated with the fluvial environment adjacent to the areas where *Attaleo maripae – Iryantherion laevis* predominates, whose geomorphological units are influenced by the main tributaries of the Guaviare and Orinoco rivers.

 doi:10.20944/preprints202604.1593.v1

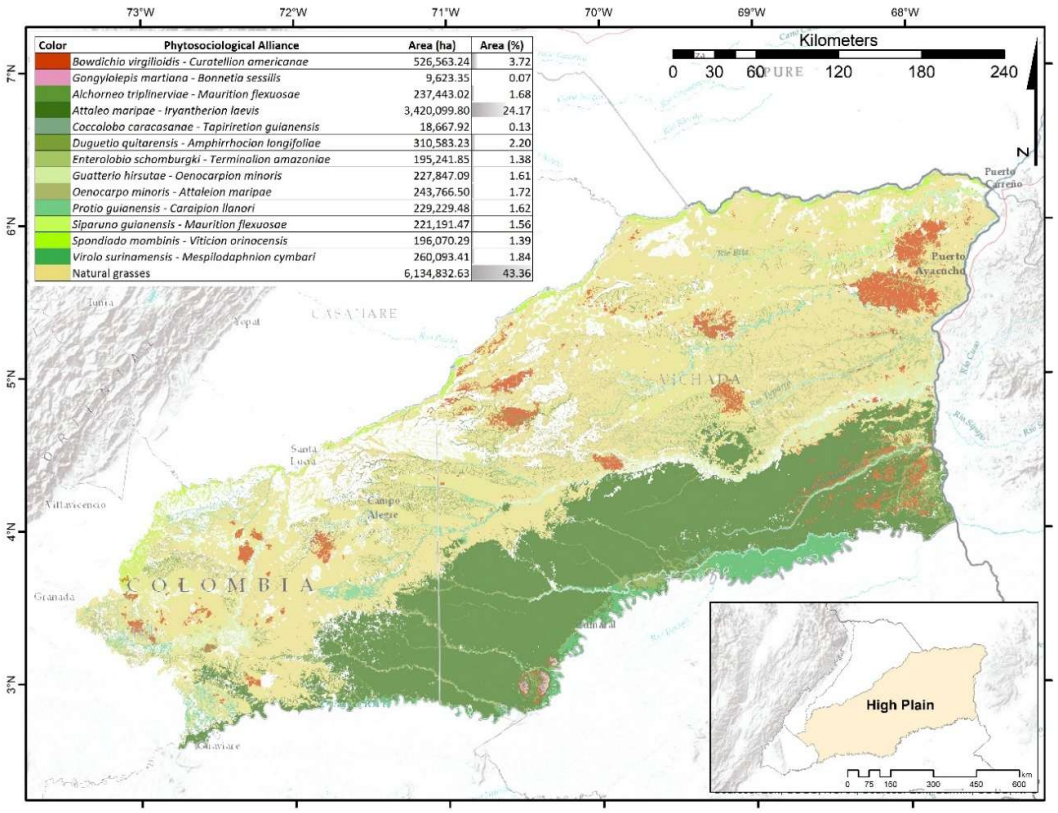

Figure 4. Spatial distribution and area of forests phytosociological alliances in the High Plain of the Colombian Orinoquia.

The formations of intermediate representation in the High Plain are predominantly associated with narrow fluvial units and denudational environments. *Virolo surinamensis – Mespilodaphnion cymbari* is located in the fluvial environment of the Guaviare River and its tributaries Siare, Iteviare, and Uva; *Oenocarpo minoris – Attaleion maripae* occupies narrow fluvial units adjacent to residual hilly plains of the Tuparrito stream and the Vichada and Tuparro rivers, as well as peneplains and hills near the Melúa, Muco, Elvita, and Tomo rivers and the upper basin of the Tuparro River; *Alchorneo triplinerviae – Maurition flexuosae* is distributed over dissected hills in the upper basins of the Melúa and Vichada rivers, highly dissected hills near the Cumaral, Cumachabo, and Rubiales streams and the Manacacías, Planas, Tillava, and Guarrojo rivers, peneplains associated with the Muco and Tomo rivers, and residual hilly plains near the Bita and Tomo rivers; *Protio guianensis – Caraipion llanori* occupies fluvial units of the denudational environment in the vicinity of the Ovejas stream, hills in the upper basin of the Manacacías River, highly dissected hills between the Meta and Yucao rivers, and floodplains associated with the Tomo River; *Guatterio hirsutae – Oenocarpion minoris* is distributed over fluvial units of the Manacacías and Vichada rivers; and *Siparuno guianensis – Maurition flexuosae* occupies narrow fluvial units over hills influenced by the Cuamaral, Melúa, Yucao, and Manacacías rivers and the middle basin of the Planas River, the peneplain of the upper basin of the Muco River, hilly plains in the middle basins of the Tomo and Tuparro rivers, and the tributaries of the Bita River and the Liqui stream.

The formations with lesser representation in the High Plain include *Spondiado mombinis – Viticion orinocensis*, associated with the fluvial units of the Meta, Juriepe, and Bita rivers; *Enterolobio schomburgki – Terminalion amazoniae*, occurring in the fluvial environment of the Orinoco, Tuparro, Tomo, Mesetas, and Guio rivers and their minor tributaries; *Coccolobo caracasanae – Tapiririetion guianensis*, in the fluvial environment of the Meta River; the low forests of *Bowdichio virgilioidis – Curatellion americanae*, distributed primarily over the inselbergs near the Mapiripana rapids on the

 doi:10.20944/preprints202604.1593.v1

Guaviare River, fill-spill plains, and hilly plains along the eastern margin of the Orinoco River, and the Matavení, Mono, and Fruta streams in the southwestern extreme of the High Plain; and the shrublands of *Gongylolepis martiana – Bonnetia sessilis*, restricted to the inselbergs near the Mapiripana rapids on the Guaviare River.

Taken together, the results reveal marked contrasts in forest cover, formation diversity, and degree of anthropic transformation across the four subregions of the Colombian Orinoquia. Forest cover ranges from 10.95% in the Floodplain and 12.51% in the Foothills — the most heavily transformed subregions, where cattle ranching, monocultures, and agricultural expansion have altered the majority of natural covers — to 39.30% in the High Plain and 55.22% in La Macarena, where anthropic transformation remains comparatively lower at 13.55% and 39.38%, respectively. Formation diversity follows a similar gradient, increasing from six formations in the Foothills to eleven in the High Plain, which concentrates the greatest phytosociological complexity of the region. Across all subregions, the distribution of formations is consistently structured by geomorphological environment — fluvial, denudational, structural, and aeolian units — reflecting the primacy of physiographic factors as spatial determinants of forest composition. The pronounced asymmetry in territorial occupation, where *Attaleo maripae – Iryantherion laevis* alone accounts for nearly 15% of the total forested area, contrasts with the relatively equitable distribution of the remaining alliances and underscores the physiognomic and floristic heterogeneity that characterizes the forests of the Colombian Orinoquia.

3. Discussion

This study characterized the geographic distribution of current vegetation in the Colombian Orinoquia through an empirical-statistical modeling approach, based on the relationship between stacked multidimensional image data — comprising optical and SAR-derived spectral variables, geomorphological units, and bioclimatic factors as predictors — and phytosociological forest alliances as the response variable. The integration of multi-source and multi-thematic data was key to discriminating vegetation types, providing complementary information on the geometry and texture of vegetation units and reducing the uncertainty associated with structural and spectral similarities [49,66,73,74]. The validated classifications identified 24 phytosociological alliances or geobotanical formations distributed across approximately 7,565,696 ha of forest cover, representing 34.63% of the region. The results reveal marked contrasts in forest cover, formation diversity, and degree of anthropic transformation across the four subregions, with the High Plain concentrating the greatest phytosociological complexity and *Attaleo maripae – Iryantherion laevis* emerging as the dominant formation at the regional scale. Collectively, these findings demonstrate that the spatial organization of forest vegetation in the Colombian Orinoquia is primarily structured by the environmental complexes and its associated edaphic-hydrological regimes, with anthropic transformation constituting the principal driver of forest cover reduction in the most accessible subregions.

The spatial discrimination of forests presents broad room for improvement through the integration of data from diverse sensors and thematic sources, such as those considered here; moreover, expanding the spectral and thematic resolution through multidimensional imagery could further improve overall accuracy and reduce variance in classifications [75,76]. Classification depends on the quality of training samples [77,78], which are derived from field surveys and reflect the spectral and landscape variability of forests. Likewise, balanced samples across thematic classes, incorporated through K-means pre-classification, increase accuracy and reduce commission and omission errors [79,80]. Although the initial K-means classification for defining training areas is useful for establishing sample representativeness, future studies could consider stratified sampling designs for selecting balanced training data based on prior thematic cartography [78,81]. Additionally, future studies could explore other capabilities of Random Forest, as this technique allows the variables included to be ranked according to their relevance in discriminating vegetation types, which could prove useful for incorporating new variables or refining those considered in the present study [56,82].

 doi:10.20944/preprints202604.1593.v1

Regarding the optical sensor, the use of the annual per-pixel median could reduce the phenological influence associated with seasonal alternation, thereby improving classification precision [78]. However, persistent cloud cover over areas of the Foothills represents the primary limitation of the optical sensor, which may be mitigated by implementing collections with greater scene availability or by extending the image acquisition period used to construct the mosaic, although this entails a reduction in temporal resolution.

The accuracy levels achieved by the classifications, together with the integration of phytosociological field data and environmental complex variables, provide a sufficiently robust spatial foundation for ecological interpretation at the subregional scale. The distributional patterns emerging from this framework reveal the principal drivers structuring forest vegetation across the Colombian Orinoquia.

The results show that the best-preserved forest remnants are concentrated on steep terrain, dissected hills, or areas distant from the population centers of the Foothills. These territories constitute persistence refugia, where low agricultural suitability has acted as a factor of passive protection [83,84]. This observation supports the theory of remnant conservation in anthropized landscapes, where biodiversity congregates in areas marginal to production [85–87]. However, even these refugia are not exempt from impact. The sequence described — encompassing forests with altered structure due to selective logging, forest-shrubland mosaics, and those embedded in matrices of pastures or agricultural areas — constitutes a clear gradient of ecological degradation. This continuum may be interpreted as a regressive succession driven by the intensity and frequency of human intervention [87,88]. Thus, the shrubland strips surrounding degraded forests should not be interpreted a priori as merely ruderal vegetation series, as they may represent stages of various successional trajectories — early and intermediate — maintained by recurrent and constant disturbances [89,90].

The identification of clearly dominant alliances that constitute key catenary and defining elements in the region — such as *Attaleo maripae – Iryantherion laevis* in the Vichada–Guaviare interfluve and *Brosimo lactescentis – Euterpion precatoriae* in the Meta plains — suggests that current ecological conditions favor their establishment as climax elements in those areas, under the prevailing edaphic-hydrological regimes of their respective physiographic units. The spatial segregation of phytocoenoses is demonstrably non-random: alliances such as *Spondiado mombinis – Viticion orinocensis* and *Duguetio quitarensis – Amphirrhocion longifoliae* are intimately linked to floodplains and active fluvial environments, reflecting the broad and dynamic alluvial processes of the region. Conversely, alliances such as *Ocoteo cernuae – Viticion orinocensis* and *Chamaedoreo pinnatifrondis – Sloaneion brevispinae* are restricted to denudational and structural environments of slopes and massifs, reflecting a clear association with radically distinct soil and drainage conditions. It is therefore suggested that drainage networks exert a significant influence on the phytosociological arrangement of forests in the region. These geomorphological factors confirm that, together with mesoclimatic conditions, the environmental gradient present in each physiographic unit constitutes the primary modulator of the considerable beta diversity observed [91–94].

The patterns documented here are consistent with previous studies that highlight the Orinoquía as a region of transition and high beta heterogeneity [6,95–98]. The identification of alliances such as *Protio guianensis – Caraipion llanori* and *Alchorneo triplinerviae – Maurition flexuosae* in highly localized environments enriches the phytosociological catalogue of Neotropical savannas and refines the mapping of units previously described in more general terms [99–101]. These findings advance the classical understanding that emphasized primarily the flooding gradient; the present results demonstrate that the geomorphological gradient — fluvial, denudational, and structural — constitutes an organizing axis of equal or greater importance for explaining not only the composition but also the ecogeographical extent of phytocoenoses at the subregional scale [92].

The present study contributes a spatially explicit and phytosociologically grounded characterization of forest vegetation in the Colombian Orinoquia, advancing beyond previous land cover approaches by resolving 24 alliances or geobotanical formations whose distribution is governed

 doi:10.20944/preprints202604.1593.v1

by the interplay of geomorphological, and bioclimatic factors. Understanding vegetation patterns in megadiverse countries is critical for addressing global conservation challenges, providing an essential foundation for wildlife habitat studies [102], species and community distribution modeling [59,103,104], identification of high conservation value areas [36,105], assessment of threats and disturbance effects on biodiversity [33,106], protection and sustainable management of forest resources [74], and the biophysical estimation of environmental supply in territories, as well as the guidance of restoration, mitigation, and ecological compensation processes based on reliable information on dominant plant species [1]. These results therefore provide an empirically validated cartographic framework that can directly inform biodiversity assessments, ecosystem service valuation, and natural capital management at the regional scale — needs that current land cover surrogates used in Colombian conservation planning have been insufficient to address.

4. Materials and Methods

4.1. Study Area

The Colombian-Venezuelan Llanos constitute the second largest expanse of Neotropical savannas (≈532,000 km²) [107,108]. This region, of notable ecological complexity and floristic diversity, extends in Colombia from the Foothills of the Eastern Cordillera to the Orinoco River, encompassing 233,546 km² [93]. Its geographic boundaries are demarcated by the Arauca River (north), the Orinoco River (east), the Guaviare River (south), and the Guayabero River basin (west) [109]. From a geomorphological perspective, two principal units are distinguished: the well-drained Orinoquia (east of the Meta River), characterized by dissected high plains and hills; and the poorly drained Orinoquía (west of the Meta River), dominated by alluvial and aeolian plains. Likewise, four physiographic units are recognized: the Foothills, the Flood/Aeolian Plain, the High Plain, and La Macarena [6,9,57,110].

4.2. Physiographic Setting [93,94]

The physiographic delimitation was based on the hydrographic zoning of Colombia [111] and the NASA SRTM v.3 digital elevation model (30 m) [112] available in Google Earth Engine. The Foothills was delimited on its eastern and western flanks using altitudinal thresholds defined according to the hydrographic basins present. South of the Meta River, in the Guamal River basin, an upper threshold of 575 m and a lower threshold of 350 m were established. North of the Meta River, altitudinal ranges were differentiated by basin: 675–200 m for the Meta and Pauto rivers, 600–200 m for the Casanare River, 425–200 m for the Cravo Sur River, and 375–175 m for the Arauca River. At its northern extreme, the boundary corresponds to the Arauca River, while to the south it is defined by the Ariari River basin. La Macarena was delimited to the west by altitudinal thresholds of 575 m in the Guayabero River basin and 775 m in the Guaviare River basin; to the north and east by the boundaries of the Ariari River basin; and to the south by the Guayabero River and the limits of its basin. The Floodplain was bounded to the west by the Foothills, to the north by the Arauca River, to the east by the international border with Venezuela, and to the south by the Meta River. The High Plain, in turn, was delimited to the west by the Foothills and La Macarena, to the north by the Meta River, to the east by the Orinoco River, and to the south by the Guaviare River (Figure 5).

 doi:10.20944/preprints202604.1593.v1

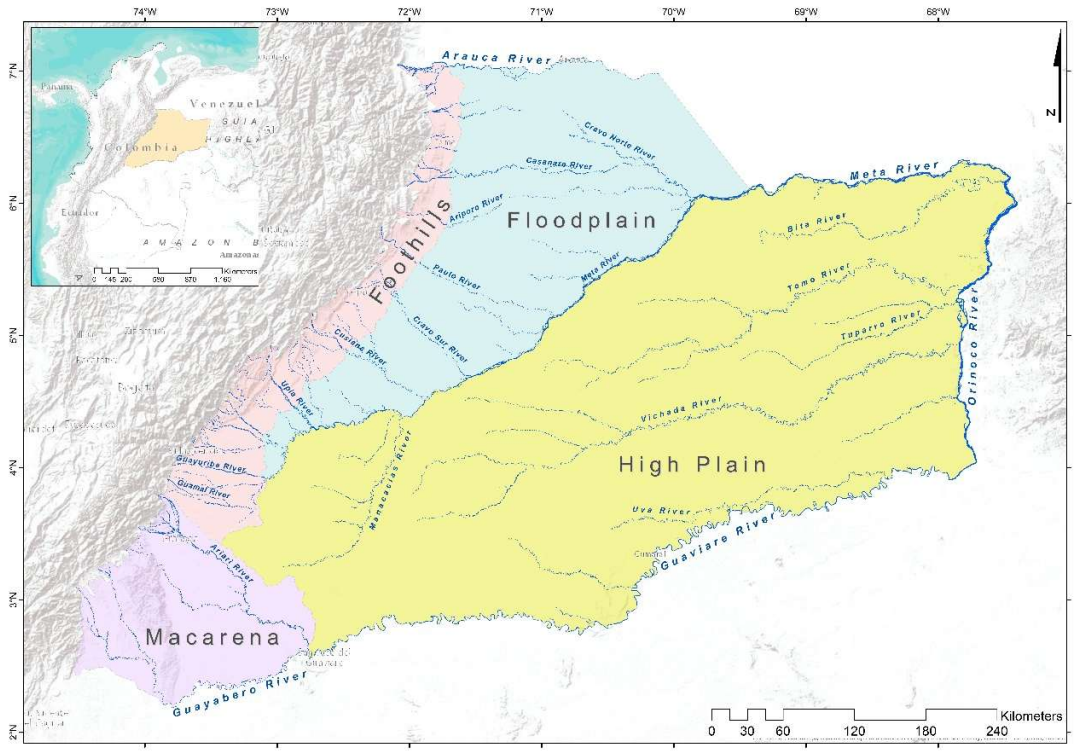

Figure 5. Spatial context of the study area, including physiographic units and the major drainage systems.

4.3. Modelling Framework and Data Training

The analysis was based on an empirical-statistical model designed to quantify the relationship between predefined phytosociological units, used as the response variable, and a set of bioclimatic predictors derived from WorldClim [113], as well as geomorphological predictors [93] and spectral predictors obtained from Landsat-8 and Sentinel-1 imagery. Unsupervised (K-means) and supervised (Random Forest) classification algorithms were applied to model the distribution patterns. The former defined training areas and the latter generated the spatial classification.

Training areas were defined using 178 forest vegetation surveys conducted in the Colombian Orinoquía; the geographic location and main attributes of these vegetation surveys are available in Minorta et al. (2026), whose syntaxonomic classification was previously established by Minorta-Cely et al. (2023a, 2023b). The phytosociological classification comprises the following syntaxonomic units: Class *Maquiro coriaceae–Copaiferetea pubiflorae*, encompassing the following orders: *Brosimo lactescentis–Oenocarpetalia minoris* (three alliances), *Iryanthero laevis–Oenocarpetalia batauae* (two alliances), *Alchorneo discoloris–Protietalia llanori* (five alliances), *Alibertio edulis–Mabeetalia trianae* (two alliances), and *Ocoteo bofo–Mabeetalia trianae* (three alliances). Class *Brosimo lactescentis–Eschweileretea subglandulosae*, including the orders: *Mabeo nitidae–Mespilodaphnetalia cymbari* (two alliances), and *Phenakospermo guianensis–Minquartietalia guianensis* (one alliance). Class *Jacarando copaiae–Luehetea seemani*, comprising the order: *Pouterio stipitatae–Terminalietalia amazoniae* (two alliances).

4.4. Data Collection and Processing

The detailed procedures for the acquisition and processing of input data are available in Niño et al. (2023, 2025, 2026):

Geomorphology. The geomorphological model integrated two L-band SAR polarizations and five parameters considered fundamental terrain descriptors [117,118]: (i) HH/HV polarizations obtained from the ALOS PALSAR 2022 annual mosaic (Global PALSAR-2/PALSAR collection, available in GEE), to which speckle correction was applied using a 50 m focal mean filter [76,119]; (ii) the NASA

 doi:10.20944/preprints202604.1593.v1

SRTM v.3 DEM, from which cartographic layers of slope, aspect, and convexity were derived; (iii) slope, expressed as a percentage of inclination; (iv) aspect, defined as the azimuthal orientation of the slope in degrees relative to north; (v) convexity, calculated from the relative elevation of a seven-pixel moving window with respect to its neighborhood, classified as concave (elevation lower than surroundings), convex (higher), or flat (similar); and (vi) surface roughness, estimated using the local variance of slope within seven-pixel moving windows.

Adjusted Potential Evapotranspiration. The adjusted potential evapotranspiration cartographic layer describes the transfer of liquid water to the atmosphere in the form of vapor, integrating both evaporation from open surfaces and plant transpiration [120]. At the regional scale, it constitutes an indicator of climatically relevant aspects such as water balance, vegetation productivity, and biodiversity [4,121]. Its calculation followed the Thornthwaite method [122] and included: (i) mean monthly temperature; (ii) the annual heat index, derived from monthly values as a measure of accumulated thermal energy; and (iii) the α parameter, a function of the heat index and an estimator of atmospheric moisture retention capacity. At regional and local scales, topography influences the distribution of solar radiation and, consequently, evapotranspiration. To obtain an adjusted estimate, a correction was applied that accounts for the number of days per month and the daily sunshine hours as a function of latitude and topography, calculated using the GRASS r.sun.insoltime algorithm [123], based on the NASA SRTM v.3 DEM at 30 m resolution available in GEE. Finally, the adjusted annual potential evapotranspiration was obtained by summing the corrected monthly values.

Ombrothermic index (annual and dry quarter). These indices establish a direct relationship between precipitation and temperature, providing an estimate of water availability as limited by evapotranspiration losses or by the reduction in rainfall efficiency with increasing temperature [23]. Their calculation included, for both the annual period and the dry quarter, positive precipitation and positive temperature.

Thermicity index. This index weights the intensity of extreme temperatures as a limiting factor for vegetation development [124]. Its calculation included: (i) mean annual temperature; (ii) the mean of minimum temperatures of the coldest month; and (iii) the mean of maximum temperatures of the coldest month.

Sentinel-1 Mosaic. This mosaic was generated from the dual-polarization C-band SAR GRD collection, preprocessed, calibrated, and orthorectified using the Sentinel-1 Toolbox, including ground range detection, thermal noise removal, radiometric calibration, topographic correction with the SRTM (30 m), and conversion to logarithmic decibel units [125]. The processing of 2022 imagery in GEE comprised: (i) selection of the interferometric wide swath mode; (ii) filtering by ascending, descending, or both orbital directions depending on topography; (iii) filtering by VV and VH polarizations; (iv) selection of data at 10 m spatial resolution; (v) clipping to the area of interest loaded as an Asset in GEE; (vi) alternating selection of VV and VH bands; (vii) temporal filtering for the full year; (viii) mosaic composition from both bands; and (ix) application of a 50 m circular focal mean filter to reduce speckle noise [94].

Landsat-8 Mosaic. This mosaic was generated from 2022 imagery of the USGS Landsat 8 Surface Reflectance Tier 1 collection, which includes bands from the visible spectrum (RGB), near-infrared (NIR), and shortwave infrared (SWIR), useful for vegetation differentiation [126–128]. These data are atmospherically and thermally corrected using the OLI/TIRS sensor and the LaSRC software [129]. Additionally, the Normalized Difference Vegetation Index (NDVI), calculated from the red and NIR bands, was incorporated to reduce the effects of illumination, topographic heterogeneity, and soil reflectance [80]. Processing in GEE included: (i) masking of clouds, shadows, and cirrus in each scene, generating a binary image that excluded affected pixels from the mosaic computation; (ii) rescaling of digital values to reflectance units; (iii) calculation of the median of unmasked pixels; and (iv) calculation of the NDVI and its stacking with the remaining bands.

 doi:10.20944/preprints202604.1593.v1

4.5. Definition of Training Areas

Training areas were delineated through unsupervised classification using the K-means algorithm in GEE, based on stacked image data and the spatial location of vegetation alliances identified in the field (vegetation survey protocols). The procedure included: (i) pixel sampling according to geometry, scale, and required quantity; (ii) training of the algorithm with the number of vegetation alliances plus four general cover types (grassland, agricultural use, urban areas, and water bodies); (iii) classification of the multidimensional image into a single-band raster with cluster identifiers; and (iv) export at a spatial resolution of 30 m. Raster values not corresponding to natural forests were reclassified as "NoData" and generalized to a scale of 5 ha. This procedure groups pixels into minimum homogeneous areas, replacing values of lesser representativeness with those of adjacent groups that reach the established threshold. The generalization process included: (i) thematic aggregation, which groups adjacent similar pixels using a focal majority filter applied to a 2 × 2 moving window; (ii) clump, which identifies groups of contiguous pixels of each thematic class according to the number of adjacent pixels; and (iii) eliminate, which iteratively applies a focal majority filter (defined at 5 ha), replacing pixel groups below the threshold with the values of surrounding areas that meet the required pixel count. Finally, the generalized thematic raster was vectorized into polygon features, and areas with spatial coincidence with vegetation sampling records, represented as point geometries, were identified [94].

4.6. Random Forest Classifier Configuration

The configuration was based principally on the calculation of the optimal number of decision trees and training variables: (i) generation of samples from the multidimensional image and training polygons; (ii) partitioning of the dataset into 70% for prediction and 30% for validation [44]; (iii) iteration with different numbers of trees to estimate accuracy without overfitting [56,130]; (iv) configuration of the classifier with the optimal value identified; (v) training with 70% of the data and execution with numerical attributes and stacked bands; and (vi) validation with the remaining 30%, calculation of the confusion matrix, and generation of accuracy curves by number of decision trees. The final classification, also executed in GEE, employed the optimal number of decision trees and the same training variables [58]. The result was exported as a raster at 30 m resolution, generalized to a minimum mapping unit of 5 ha, and vectorized. Confusion matrices, overall accuracy, producer and user accuracies, and the Kappa coefficient were calculated. Figure 6 presents the methodological synopsis employed to model the current distribution of forests in the Orinoquia.

 doi:10.20944/preprints202604.1593.v1

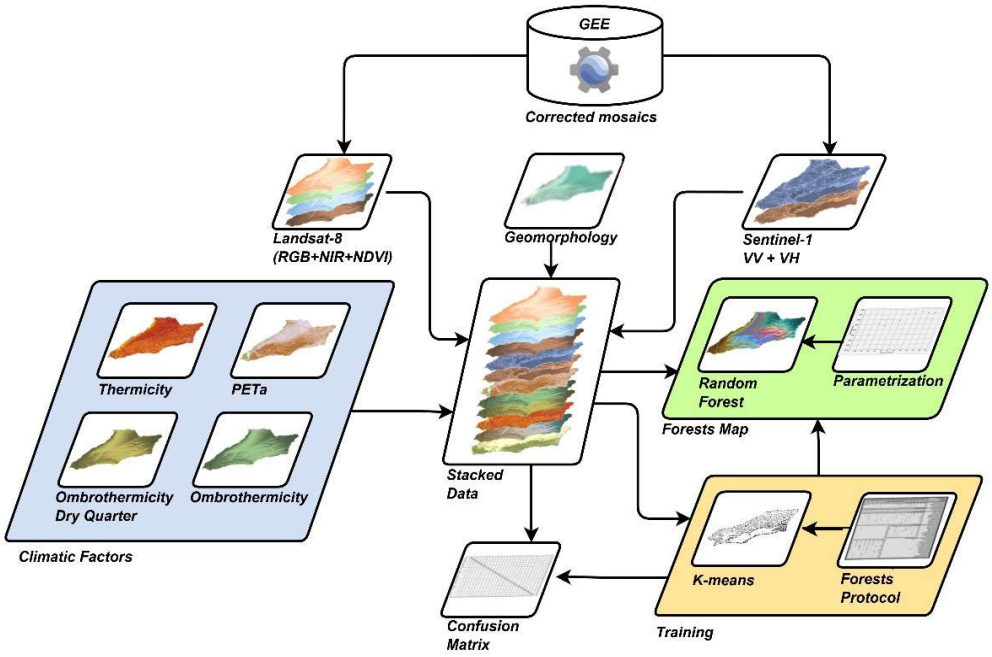

Figure 6. Methodological workflow for the spatial modeling of forests in the Colombian Orinoquia. The process integrates multi-source data and machine learning to classify and validate forests areas.

5. Conclusions

The present study demonstrates that the integration of phytosociological field data, environmental complex variables, and multi-sensor satellite imagery within a Random Forest classification framework constitutes a robust and replicable approach for characterizing forest vegetation distribution at the regional scale. The 24 phytosociological alliances or geobotanical formations identified across the Colombian Orinoquia represent a significant advance over existing land cover surrogates, resolving the floristic and physiognomic complexity of approximately 7,565,696 ha of forest cover with high spatial accuracy and thematic detail.

The spatial organization of these formations is governed primarily by the geomorphological gradient — fluvial, denudational, and structural — and its associated edaphic-hydrological regimes, with mesoclimatic factors operating as complementary modulators of beta diversity across subregions. Anthropic transformation, driven predominantly by cattle ranching, agricultural expansion, and selective logging, constitutes the principal threat to forest cover, particularly in the Piedmont and Alluvial Plain subregions, where the most accessible and fertile environments have been most extensively altered. The persistence of forest remnants in areas of low agricultural suitability underscores both the passive protective role of topographic marginality and the urgent need for active conservation strategies in these refugia.

The cartographic framework produced here provides an empirically validated foundation for biodiversity assessments, ecosystem service valuation, habitat modeling, and ecological restoration planning in the Colombian Orinoquia. The methodological approach demonstrated is directly transferable to other subregions of the Orinoquia and to analogous Neotropical landscapes where detailed vegetation mapping remains a critical and unresolved challenge for conservation science and natural capital management.

 doi:10.20944/preprints202604.1593.v1

Author Contributions: Conceptualization, methodology and formal analysis L.N; investigation L.N, V.M.-C., J.O.R.-C., D.G.-C. and D.S.-M.; data curation L.N, V.M.-C., J.O.R.-C., D.G.-C. and D.S.-M.; writing—original draft preparation L.N, V.M.-C., J.O.R.-C., D.G.-C. and D.S.-M.; writing—review and editing L.N, V.M.-C., J.O.R.-C., D.G.-C. and D.S.-M.; visualization L.N, V.M.-C., J.O.R.-C., D.G.-C. and D.S.-M. All authors have read and agreed to the published version of the manuscript.

Funding: This research received no external funding.

Data Availability Statement: All data supporting the reported results are included or cited in the paper.

Acknowledgments: We would like to thank Francisco Castro-Lima, Gerardo Aymard and Francisco Mijares for their vegetation plots, as well as their support during fieldwork and the taxonomic identification of species.

Conflicts of Interest: The authors declare no conflicts of interest.

References

1. Ibarra, G.; González, M.; Martínez, M.; Meave, J. From Vegetation Ecology to Vegetation Science: Current Trends and Perspectives. *Bot. Sci.* **2022**, 137–174, doi:10.17129/botsci.3171.
2. Salovaara, K.; Thessler, S.; Malik, R.; Tuomisto, H. Classification of Amazonian Primary Rain Forest Vegetation Using Landsat ETM+ Satellite Imagery. *Remote Sens. Environ.* **2005**, *97*, 39–51, doi:10.1016/j.rse.2005.04.013.
3. Cavender-Bares, J.; Gamon, J.; Townsend, P. The Use of Remote Sensing to Enhance Biodiversity Monitoring and Detection: A Critical Challenge for the Twenty-First Century. In *Remote Sensing of Plant Biodiversity*; Cavender-Bares, J., Gamon, J., Townsend, P., Eds.; Springer: Cham, Switzerland, 2020; pp. 1–12.
4. Rietkerk, M.; Brovkin, V.; van Bodegom, P.; Claussen, M.; Dekker, S.; Dijkstra, H.; Goryachkin, S.; Kabat, P.; van Nes, E.; Neutel, A.; et al. Local Ecosystem Feedbacks and Critical Transitions in the Climate. *Ecol. Complex.* **2011**, *8*, 223–228, doi:10.1016/j.ecocom.2011.03.001.
5. Whittaker, R. Gradient Analysis of Vegetation. *Biol. Rev.* **1967**, *42*, 207–264, doi:10.1111/j.1469-185X.1967.tb01419.x.
6. Blydenstein, J. Tropical Savanna Vegetation of the Llanos of Colombia. *Ecology* **1967**, *48*, 1–15.
7. Dugand, A. Plantae Praesertium Maypurenses a Humboldtio et Bonplandio in Ripa Occidentali Fluminis Orinoco Lectae Ideoque Ad Floram Colombiensem Referendar. *Acad. Colomb. Ciencas Exactas Físicas y Nat.* **1956**, *9*, 315–324.
8. FAO *La Vegetación Natural y La Ganadería*; Organización de las Naciones Unidas para la Agricultura y la Alimentación FAO: Roma, Italia, 1965;
9. Goosen, D. División Fisiográfica de Los Llanos Orientales. *Rev. Nac. Agric.* **1963**, *55*, 39–41.
10. Rangel-Ch, J.O.; Sánchez-C, H.; Lowy-C, P.; Aguilar-P, M.; Castillo, A. Región de La Orinoquia. In *Colombia Diversidad Biótica Vol. I*; Rangel-Ch, J.O., Ed.; Universidad Nacional de Colombia, Instituto de Ciencias Naturales: Bogotá, Colombia, 1995; pp. 239–254.
11. Jetz, W.; Cavender-Bares, J.; Pavlick, R.; Schimel, D.; Davis, F.; Asner, G.; Guralnick, R.; Kattge, J.; Latimer, A.; Moorcroft, P.; et al. Monitoring Plant Functional Diversity from Space. *Nat. plants* **2016**, *2*, 16024, doi:10.1038/nplants.2016.24.
12. Xie, Y.; Sha, Z.; Yu, M. Remote Sensing Imagery in Vegetation Mapping: A Review. *J. Plant Ecol.* **2008**, *1*, 9–23.
13. Guisan, A.; Thuiller, W. Predicting Species Distribution: Offering More than Simple Habitat Models. *Ecol. Lett.* **2005**, *8*, 993–1009, doi:10.1111/j.1461-0248.2005.00792.x.
14. Guisan, A.; Zimmermann, N. Predictive Habitat Distribution Models in Ecology. *Ecol. Modell.* **2000**, *135*, 147–186.
15. Austin, M. Searching for a Model for Use in Vegetation Analysis. *Vegetatio* **1980**, *42*, 11–21.
16. Austin, M. Continuum Concept, Ordination Methods, and Niche Theory. *Annu. Rev. Ecol. Syst.* **1985**, *16*, 39–61.
17. Austin, M.; Smith, T. A New Model for the Continuum Concept. *Vegetatio* **1989**, *83*, 35–47.

 doi:10.20944/preprints202604.1593.v1

18. Guisan, A.; Weiss, S.; Weiss, A. GLM versus CCA Spatial Modeling of Plant Species Distribution. *Plant Ecol.* **1999**, *143*, 107–122.
19. Dymond, C.; Johnson, E. Mapping Vegetation Spatial Patterns from Modeled Water, Temperature and Solar Radiation Gradients. *J. Photogramm. Remote Sens.* **2002**, *57*, 69–85, doi:10.1016/S0924-2716(02)00110-7.
20. Stewart, S.; Elith, J.; Fedrigo, M.; Kasel, S.; Roxburgh, S.; Bennett, L.; Chick, M.; Fairman, T.; Leonard, S.; Kohout, M.; et al. Climate Extreme Variables Generated Using Monthly Time-Series Data Improve Predicted Distributions of Plant Species. *Ecography (Cop.).* **2021**, *44*, 1–14, doi:10.1111/ecog.05253.
21. Zimmermann, N.; Yoccoz, N.; Edwards, T.; Meier, E.; Thuiller, W.; Guisan, A.; Schmatz, D.; Pearman, P. Climatic Extremes Improve Predictions of Spatial Patterns of Tree Species. In Proceedings of the Biogeography, Changing Climates and Niche Evolution; Proceedings of the National Academy of Sciences: Irvine, CA (USA), 2009; pp. 19723–19728.
22. Londe, V.; Gomes, P.; Martins, F. The Role of Edaphic Differentiation on Life Zones, Vegetation Types, β-Diversity, and Indicator Species in Tropical Dry Forests. *Plant Soil* **2023**, 73–588, doi:10.1007/s11104-023-06249-3.
23. Rivas-Martínez, S.; Rivas, S.; Penas, A. Worldwide Bioclimatic Classification System. *Glob. Geobot.* **2011**, *1*, 1–634, doi:10.5616/gg110001.
24. Bocco, G.; Mendoza, M.; Velázquez, A. Remote Sensing and GIS-Based Regional Geomorphological Mapping—a Tool for Land Use Planning in Developing Countries. *Geomorphology* **2001**, *39*, 211–219.
25. Costa, M.; Cegarra, A.; Lugo, L.; Lozada, J.; Guevara, J.; Soriano, P. The Bioclimatic Belts of the Venezuelan Andes in the State of Merida. *Phytocoenologia* **2007**, *37*, 711–738, doi:10.1127/0340-269X/2007/0037-0711.
26. Gavilán, R. The Use of Climatic Parameters and Indices in Vegetation Distribution. A Case Study in the Spanish Sistema Central. *Int J Biometeorol* **2005**, *50*, 111–120, doi:10.1007/s00484-005-0271-5.
27. Gopar-Merino, L.; Velázquez, A.; Giménez, J. Bioclimatic Mapping as a New Method to Assess Effects of Climatic Change. *Ecosphere* **2015**, *6*, 1–12, doi:10.1890/ES14-00138.1.
28. Macías, M.; Peinado, M.; Giménez, J.; Aguirre, J.; Delgadillo, J. Clasificación Bioclimática de La Vertiente Del Pacífico Mexicano y Su Relación Con La Vegetación Potencial. *Acta Bot. Mex.* **2014**, *109*, 133–165.
29. Navarro, G. Contribución a La Clasificación Ecológica y Florística de Los Bosques de Bolivia. *Rev. Boliv. Ecol. y Conserv. Ambient.* **1997**, *2*, 3–37.
30. Rivas-Martínez, S.; Cantó, P.; Pizarro, J.; Izquierdo, J.; Rivas-Sáenz, S.; Molero, J.; Marfil, J.; Penas, A.; Herrero, L.; Díaz, T.; et al. Advances in Geobotany and New Tools in Biogeographic and Bioclimatic Maps: Sierra de Guadarrama National Park. *Int. J. Geobot. Res.* **2021**, *10*, 91–110, doi:10.5616/ijgr 211006.
31. Montesinos, S.; Fernández, L.; De Veer, D.; Cifuentes, N. Sentinel 2A En El Seguimiento Del Jacinto de Agua En La Cuenca Media Del Río Guadiana. In Proceedings of the XVII Congreso de la Asociación Española de Teledetección: Nuevas plataformas y sensores de teledetección; Ruiz, L., Estornell, J., Erena, M., Eds.; Universitat Politècnica de València: Murcia, España, 2017; pp. 259–262.
32. Stone, T.; Schlesinger, P.; Houghton, R.; Woodwell, G. A Map of the Vegetation of South America Based on Satellite Imagery. *Photogramm. Eng. Remote Sens.* **1994**, *60*, 541–551.
33. Díaz, S.; Cabido, M.; Casanoves, F. Plant Functional Traits and Environmental Filters at a Regional Scale. *J. Veg. Sci.* **1998**, *9*, 113–122, doi:10.2307/3237229.
34. Schweiger, A. Spectral Field Campaigns: Planning and Data Collection. In *Remote Sensing of Plant Biodiversity*; Cavender-Bares, J., Gamon, J., Townsend, P., Eds.; Springer: Cham, Switzerland, 2020; pp. 385–423.
35. Tuomisto, H.; Poulsen, A.; Ruokolainen, K.; Moran, R.; Quintana, C.; Celi, J.; Cañas, G. Linking Floristic Patterns with Soil Heterogeneity and Satellite Imagery in Ecuadorian Amazonia. *Ecol. Appl.* **2003**, *13*, 352–371, doi:10.1890/1051-0761(2003)013[0352:LFPWSH]2.0.CO;2.
36. Martin, R. Lessons Learned from Spectranomics: Wet Tropical Forests. In *Remote Sensing of Plant Biodiversity*; Cavender-Bares, J., Gamon, J., Townsend, P., Eds.; Springer: Cham, Switzerland, 2020; pp. 105–120.
37. Reichstein, M.; Bahn, M.; Mahecha, M.; Kattge, J.; Baldocchi, D. Linking Plant and Ecosystem Functional Biogeography. *Proc Natl Acad Sci* **2014**, *111*, 13697–13702, doi:10.1073/ pnas.1216065111.

 doi:10.20944/preprints202604.1593.v1

38. Paradella, W.; Santos, A.; Veneziani, P.; Cunha, E. Radares Imageadores Nas Geociências: Status e Perspectivas. In Proceedings of the Anais XII Simpósio Brasileiro de Sensoriamento Remoto; Instituto Nacional de Pesquisas Espaciais INPE: Goiânia, Brasil, 2005; pp. 1847–1854.
39. Topouzelis, K.; Psyllos, A. Oil Spill Feature Selection and Classification Using Decision Tree Forest on SAR Image Data. *ISPRS J. Photogramm. Remote Sens.* **2012**, 135–143, doi:10.1016/j.isprsjprs.2012.01.005.
40. Castañeda, C.; Ducrot, D. Land Cover Mapping of Wetland Areas in an Agricultural Landscape Using SAR and Landsat Imagery. *J. Environ. Manage.* **2009**, *90*, 2270–2277, doi:10.1016/j.jenvman.2007.06.030.
41. Colditz, R. An Evaluation of Different Training Sample Allocation Schemes for Discrete and Continuous Land Cover Classification Using Decision Tree-Based Algorithms. *Remote Sens.* **2015**, 9655–9681, doi:10.3390/rs70809655.
42. Franklin, S.; Maudie, A.; Lavigne, M. Using Spatial Co-Occurrence Texture to Increase Forest Structure and Species Composition Classification Accuracy. *Photogramm. Eng. Remote Sensing* **2001**, *67*, 849–856.
43. Hamilton, S.; Kellndorfer, J.; Lehner, B.; Tobler, M. Remote Sensing of Floodplain Geomorphology as a Surrogate for Biodiversity in a Tropical River System (Madre de Dios, Peru). *Geomorphology* **2007**, *89*, 23–38, doi:10.1016/j.geomorph.2006.07.024.
44. Azzari, G.; Lobell, D. Landsat-Based Classification in the Cloud: An Opportunity for a Paradigm Shift in Land Cover Monitoring. *Remote Sens. Environ.* **2017**, *202*, 64–74, doi:10.1016/j.rse.2017.05.025.
45. Gorelick, N.; Hancher, M.; Dixon, M.; Ilyushchenko, S.; Thau, D.; Moore, R. Google Earth Engine: Planetary-Scale Geospatial Analysis for Everyone. *Remote Sens. Environ.* **2017**, 18–27.
46. Kumar, L.; Mutanga, O. Google Earth Engine Applications Since Inception: Usage, Trends, and Potential. *Remote Sens.* **2018**, *10*, 1–15, doi:10.3390/rs10101509.
47. Perilla, G.; Mas, J. Google Earth Engine (GEE): Una Poderosa Herramienta Que Vincula El Potencial de Los Datos Masivos y La Eficacia Del Procesamiento En La Nube. *Investig. Geográficas* **2020**, *101*, e59929, doi:10.14350/rig.59929.
48. Reiche, J.; Lucas, R.; Mitchell, A.; Verbesselt, J.; Hoekman, D.; Haarpaintner, J.; Kellndorfer, J.; Rosenqvist, A.; Lehmann, E.; Woodcock, C.; et al. Combining Satellite Data for Better Tropical Forest Monitoring. *Nat. Clim. Chang.* **2016**, *6*, 120–122.
49. Meyer, F. Spaceborne Synthetic Aperture Radar: Principles, Data Access, and Basic Processing Techniques. In *The SAR handbook*; Flores-Anderson, A., Herndon, K., Thapa, R., Cherrington, E., Eds.; SERVIR Global Science: Huntsville, EEUU, 2019; pp. 21–44.
50. Moré-Gómez, G.; Pons, X.; Burriel-Moreno, J.; Castells-Ferré, R.; Ibàñez-Martí, J.; Roijals-Lara, X. Diferenciación de Cubiertas Forestales Para El MSCS a Partir de La Clasificación de Imágenes Landsat. *Cuad. la Soc. Española Ciencias For.* **2005**, 153–162.
51. Borrás, J.; Delegido, J.; Pezzola, A.; Pereira, M.; Morassi, G.; Camps-Valls, G. Clasificación de Usos Del Suelo a Partir de Imágenes Sentinel-2. *Rev. Teledetec.* **2017**, 55–66.
52. Niño, L. Aproximaciones Cartográficas a La Vegetación, Los Ecosistemas y Las Amenazas En Las Sabanas y Humedales de Arauca (Orinoquía Colombiana). In *Colombia Diversidad Biótica Vol. XX: Territorio sabanas y humedales de Arauca (Colombia)*; Rangel-Ch, J.O., Andrade-C, G., Jarro-F, C., Santos-C, G., Eds.; Universidad Nacional de Colombia: Bogotá, Colombia, 2019; pp. 789–807.
53. Niño, L. Aspectos Cartográficos de La Vegetación, Los Ecosistemas y Las Amenazas En La Serranía de Manacacías (Meta) Orinoquía Colombiana. In *Colombia Diversidad Biótica Vol. XVII: La región de la Serranía de Manacacías (Meta) Orinoquía colombiana*; Rangel-Ch, J.O., Andrade-C, G., Jarro-F, C., Santos-C, G., Eds.; Universidad Nacional de Colombia: Bogotá, Colombia, 2019; pp. 573–600.
54. Niño, L. La Cartografía de La Vegetación, Los Ecosistemas y Las Amenazas En El Territorio de Las Selvas Transicionales de Cumaribo, Vichada (Colombia). In *Colombia Diversidad Biótica Vol. XIX: Selvas transicionales de Cumaribo (Vichada - Colombia)*; Rangel-Ch, J.O., Andrade-C, G., Jarro-F, C., Santos-C, G., Eds.; Universidad Nacional de Colombia: Bogotá, Colombia, 2019; pp. 615–636.
55. Akar, Ö.; Güngör, O. Classification of Multispectral Images Using Random Forest Algorithm. *J. Geod. Geoinf.* **2012**, *1*, 105–112, doi:10.9733/jgg.241212.1.
56. Belgiu, M.; Dragut, L. Random Forest in Remote Sensing: A Review of Applications and Futuredirections. *ISPRS J. Photogramm. Remote Sens.* **2016**, 24–31, doi:10.1016/j.isprsjprs.2016.01.011.

 doi:10.20944/preprints202604.1593.v1

57. Niño, L.; Jaramillo, A.; Villamizar, V.; Rangel-Ch, J.O. Geomorphology, Land-Use, and Hemeroby of Foothills in Colombian Orinoquia: Classification and Correlation at a Regional Scale. *Pap. Appl. Geogr.* **2023**, *9*, 295–314, doi:10.1080/23754931.2023.2189921.
58. Pal, M. Random Forest Classifier for Remote Sensing Classification. *Int. J. Remote Sens.* **2005**, *26*, 217–222, doi:10.1080/01431160412331269698.
59. Ferrier, S. Mapping Spatial Pattern in Biodiversity for Regional Conservation Planning: Where to from Here? *Syst. Biol.* **2002**, *51*, 331–363, doi:10.1080/10635150252899806.
60. Vormisto, J.; Phillips, O.; Ruokolainen, K.; Tuomisto, H.; Vázquez, R. A Comparison of Fine-Scale Distribution Patterns of Four Plant Groups in an Amazonian Rainforest. *Ecography (Cop.).* **2000**, *23*, 349–359, doi:10.1111/j.1600-0587.2000.tb00291.x.
61. McNellie, M.; Oliver, I.; Ferrier, S.; Newell, G.; Manion, G.; Griffioen, P.; White, M.; Koen, T.; Somerville, M.; Gibbons, P. Extending Vegetation Site Data and Ensemble Models to Predict Patterns of Foliage Cover and Species Richness for Plant Functional Groups. *Landsc. Ecol.* **2021**, 391–1407, doi:10.1007/s10980-021-01221-x.
62. Féret, J.; Asner, G. Mapping Tropical Forest Canopy Diversity Using High-Fidelity Imaging Spectroscopy. *Ecol. Appl.* **2014**, *24*, 1289–1296, doi:10.1890/13-1824.1.
63. Tuomisto, H.; Linna, A.; Kalliola, R. Use of Digitally Processed Satellite Images in Studies of Tropical Rain Forest Vegetation. *Int. J. Remote Sens.* **1994**, *15*, 1595–1610, doi:10.1080/01431169408954194.
64. Plourde, L.; Congalton, R. Sampling Method and Sample Placement:How Do They Affect the Accuracy OfRemotely Sensed Maps? *Photogramm. Eng. Remote Sens.* **2003**, *69*, 289–297.
65. Rosenfield, G.; Fitzpatrick-Lins, K. A Coefficient of Agreement as Ameasure of Thematic Classification Accuracy. *Photogramm. Eng. Remote Sens.* **1986**, 223–227.
66. Wiser, S.; McCarthy, J.; Bellingham, P.; Jolly, B.; Meiforth, J.; Kaitiaki, W. Integrating Plot-Based and Remotely Sensed Data to Map Vegetation Types in a New Zealand Warm-Temperate Rainforest. *Appl. Veg. Sci.* **2022**, *25*, e12695, doi:10.1111/avsc.12695.
67. Romero-Ruiz, M.; Flantua, S.; Tansey, K.; Berrio, J. Landscape Transformations in Savannas of Northern South America: Land Use/Cover Changes since 1987 in the Llanos Orientales of Colombia. *Appl. Geogr.* **2011**, *32*, 766–776, doi:10.1016/j.apgeog.2011.08.010.
68. Niño, L. Aproximación Socioeconómica Sobre La Serranía de Manacacías (Meta) Orinoquía Colombiana. In *Colombia Diversidad Biótica Vol. XVII: La región de la Serranía de Manacacías (Meta) Orinoquía colombiana*; Rangel-Ch, J.O., Andrade-C, G., Jarro-F, C., Santos-C, G., Eds.; Universidad Nacional de Colombia: Bogotá, Colombia, 2019; pp. 601–628 ISBN 978-958-783-873-2.
69. Arcila, O. Coca, Guerrilla, Colonización y Narcotráfico En La Macarena. *Rev. la Univ. Nac.* **2009**, 75–80.
70. Niño, L. Zonificación Minera Basada En La Integración de La Evaluación Ambiental Estratégica y Modelado Con Múltiples Criterios En La Región de La Macarena, Departamento Del Meta, Orinoquía Colombiana. *Rev. BIOLLANIA* **2017**, *15*, 634–666.
71. Sacristán, F. *Construyendo Agenda 21 Para El Municipio de La Macarena "Una Construcción Colectiva Para El Desarrollo Sostenible de La Amazonia Colombiana"*; Salazar, C., Ed.; Instituto Amazónico de Investigaciones Cientifícas SINCHI: Bogotá, Colombia, 2007;
72. Niño, L. Aproximación Socioeconómica Del Territorio Sabanas y Humedales de Arauca, Colombia. In *Colombia Diversidad Biótica Vol. XX: Territorio sabanas y humedales de Arauca (Colombia)*; Rangel-Ch, J.O., Andrade-C, G., Jarro-F, C., Santos-C, G., Eds.; Universidad Nacional de Colombia: Bogotá, Colombia, 2019; pp. 761–788.
73. Souza, P.; Paradella, W. Recognition of the Main Geobotanical Features along the Bragança Mangrove Coast (Brazilian Amazon Region) from Landsat TM and RADARSAT-1 Data. *Wetl. Ecol. Manag.* **2002**, *10*, 123–132.
74. Yang, Q.; Bader, M.; Feng, G.; Li, J.; Zhang, D.; Long, W. Mapping Species Assemblages of Tropical Forests at Different Hierarchical Levels Based on Multivariate Regression Trees. *For. Ecosyst.* **2023**, *10*, 100120, doi:10.1016/j.fecs.2023.100120.
75. Blaes, X.; Vanhalle, L.; Defourny, P. Efficiency of Crop Identification Based on Optical and SAR Image Time Series. *Remote Sens. Environ.* **2005**, 352–365, doi:10.1016/j.rse.2005.03.010.

 doi:10.20944/preprints202604.1593.v1

76. Waske, B.; Braun, M. Classifier Ensembles for Land Cover Mapping Using Multitemporal SAR Imagery. *ISPRS J. Photogramm. Remote Sens.* **2009**, 450–457, doi:10.1016/j.isprsjprs.2009.01.003.
77. Olofsson, P.; Foody, G.; Herold, M.; Stehman, S.; Woodcock, C.; Wulder, M. Good Practices for Estimating Area and Assessing Accuracy of Land Change. *Remote Sens. Environ.* **2014**, 42–57, doi:10.1016/j.rse.2014.02.015.
78. Polyakova, A.; Mukharamova, S.; Yermolaev, O.; Shaykhutdinova, G. Automated Recognition of Tree Species Composition of Forest Communities Using Sentinel-2 Satellite Data. *Remote Sens.* **2023**, *15*, 329, doi:10.3390/rs15020329.
79. Jin, H.; Stehman, S.; Mountrakis, G. Assessing the Impact of Training Sample Selection on Accuracy of an Urban Classification: A Case Study in Denver, Colorado. *Int. J. Remote Sens.* **2014**, *26*, 217–222, doi:10.1080/01431160412331269698.
80. Tsai, Y.; Stow, D.; Chen, J.; Lewison, R.; An, L.; Shi, L. Mapping Vegetation and Land Use Types in Fanjingshan National Nature Reserve Using Google Earth Engine. *Remote Sens.* **2018**, *10*, 1–14, doi:10.3390/rs10060927.
81. Shetty, S. Analysis of Machine Learning Classifiers for LULC Classification on Google Earth Engine, University of Twente, 2019.
82. Vega, L.; Hirata, Y.; Ventura, L.; Serrudo, N. Natural Forest Mapping in the Andes (Peru): A Comparison of the Performance of Machine-Learning Algorithms. *Remote Sens.* **2018**, *10*, 1–20, doi:10.3390/rs10050782.
83. Lopes, D.; Tsuyuki, S. Deforestation and Forest Degradation Detection in the Brazilian Amazon: A Comparative Analysis of Two Areas and Their Conservation Units. *Appl. Sci.* **2024**, *14*, 10504, doi:10.3390/app142210504.
84. Bourgoin, C.; Blanc, L.; Bailly, J.; Cornu, G.; Berenguer, E.; Oszwald, J.; Tritsch, I.; Laurent, F.; Hasan, A.; Sist, P.; et al. The Potential of Multisource Remote Sensing for Mapping the Biomass of a Degraded Amazonian Forest. *Forests* **2018**, *9*, 303, doi:10.3390/f9060303.
85. Pompeu, J.; Soler, L.; Ometto, J. Modelling Land Sharing and Land Sparing Relationship with Rural Population in the Cerrado. *Land* **2018**, *7*, 88, doi:10.3390/land7030088.
86. Zhao, J.; Cao, Y.; Yu, L. Global Change of Land-Sparing and Land-Sharing Patterns over the Past 30 Years: Evidence from Remote Sensing and Statistics. *Remote Sens.* **2021**, *13*, 5090, doi:10.3390/rs13245090.
87. Frappart, F.; Wigneron, J.; Li, X.; Liu, X.; Al-Yaari, A.; Fan, L.; Wang, M.; Moisy, C.; Le Masson, E.; Z, A.; et al. Global Monitoring of the Vegetation Dynamics from the Vegetation Optical Depth (VOD): A Review. *Remote Sens.* **2020**, *12*, 2915, doi:10.3390/rs12182915.
88. Mondragón, V.; Chilito, L.; Cabezas, C.; Macías, D. Floristic Composition and Diversity Along a Successional Gradient in Andean Montane Forests, Southwestern Colombia. *Plants* **2026**, *15*, 389, doi:10.3390/plants15030389.
89. Klink, C.; Sato, M.; Cordeiro, G.; Ramos, M. The Role of Vegetation on the Dynamics of Water and Fire in the Cerrado Ecosystems: Implications for Management and Conservation. *Plants* **2020**, *9*, 1803, doi:10.3390/plants9121803.
90. Félix, A.; Romo, J.; Hinojo, C.; Castellanos, A.; Macías, A. Analyzing Grassland Reduction and Woody Vegetation Expansion in Protected Sky Island of Northwest Mexico. *Land* **2025**, *14*, 2357, doi:10.3390/land14122357.
91. Kumar, S.; Hanan, N.; Prihodko, L.; Anchang, J.; Ross, C.; Ji, W.; Lind, B. Alternative Vegetation States in Tropical Forests and Savannas: The Search for Consistent Signals in Diverse Remote Sensing Data. *Remote Sens.* **2019**, *11*, 815, doi:10.3390/rs11070815.
92. Minorta-Cely, V.; Niño, L.; Rangel-Ch, J.O.; Sánchez-Mata, D. Environmental Factors Influencing Species Richness Expression in Grasslands of the Colombian Orinoquia. *Plants* **2024**, *13*, 3545, doi:10.3390/plants13243545.
93. Niño, L.; Jaramillo, A.; Villamizar, V.; Rangel, O.; Minorta, V.; Sánchez, D. Geomorphological Characterization of the Colombian Orinoquia. *Land* **2025**, *14*, 2438, doi:10.3390/land14122438.
94. Niño, L.; Rangel, O.; Giraldo, D.; Sánchez, D.; Minorta, V. Characterizing and Mapping the Grassland Vegetation of the Colombian Orinoquia. *Grasses* **2026**, *5*, 10, doi:10.3390/grasses5010010.

 doi:10.20944/preprints202604.1593.v1

95. Sarmiento, G.; Pinillos, M. Patterns and Processes in a Seasonally Flooded Tropical Plain: The Apure Llanos, Venezuela. *J. Biogeogr.* **2001**, *28*, 985–996, doi:10.1046/j.1365-2699.2001.00601.x.
96. Sarmiento, G.; Pinillos, M.; Silva, M.; Acevedo, D. Effects of Soil Water Regime and Grazing on Vegetation Diversity and Production in a Hyperseasonal Savanna in the Apure Llanos, Venezuela. *J. Trop. Ecol.* **2004**, *20*, 209–220, doi:10.1017/S0266467403001299.
97. Chacón, E.; Naranjo, M.; Acevedo, D. Direct and Indirect Vegetation-Environment Relationships in the Flooding Savanna of Venezuela. *Ecotrópicos* **2004**, *17*, 25–37, doi:10.13039/501100000780.
98. Beard, J. The Savanna Vegetation of Northern Tropical America. *Ecol. Monogr.* **1953**, *23*, 149–215, doi:10.2307/1948518.
99. Haase, R. Plant Communities of a Savanna in Northern Bolivia. II. Palm Swamps, Dry Grassland, and Shrubland. *Phytocoenologia* **1990**, *18*, 343–370, doi:10.1127/phyto/18/1990/343.
100. Haase, R. Plant Communities of a Savanna in Northern Bolivia. I. Seasonally Flooded Grassland and Gallery Forest. *Phytocoenologia* **1989**, *18*, 55–81, doi:10.1127/phyto/18/1989/55.
101. Menegat, H.; Silvério, D.; Mews, H.; Colli, G.; Abadia, A.; Maracahipes, L.; Gonçalves, L.; Martins, J.; Lenza, E. Effects of Environmental Conditions and Space on Species Turnover for Three Plant Functional Groups in Brazilian Savannas. *J. Plant Ecol.* **2019**, *12*, 1047–1058, doi:10.1093/jpe/rty054.
102. Salovaara, K.; Cárdenas, G.; Tuomisto, H. Forest Classification in an Amazonian Rainforest Landscape Using Pteridophytes as Indicator Species. *Ecography (Cop.).* **2004**, *27*, 689–700, doi:10.1111/j.0906-7590.2004.03958.x.
103. Foody, G. Remote Sensing of Tropical Forest Environments: Towards the Monitoring of Environmental Resources for Sustainable Development. *Int. J. Remote Sens.* **2003**, *24*, 4035– 4046, doi:10.1080/0143116031000103853.
104. Kerr, J.; Ostrovsky, M. From Space to Species: Ecological Applications for Remote Sensing. *Trends Ecol. Evol.* **2003**, *18*, 299– 305, doi:10.1016/S0169-5347(03)00071-5.
105. Gopar-Merino, L.; Velazquez, A.; González-Pérez, A.; del Río, S.; Mas, J.; Penas, A. A Coupled Cartographic Approach between Bioclimatology and Vegetation Formations of Mexico. *Veg. Classif. Surv.* **2024**, *5*, 153–164, doi:10.3897/VCS.120442.
106. Foody, G.; Cutler, M. Tree Biodiversity in Protected and Logged Bornean Tropical Rain Forests and Its Measurement by Satellite Remote Sensing. *J. Biogeogr.* **2003**, *30*, 1053–1066, doi:10.1046/j.1365-2699.2003.00887.x.
107. Aymard, G. Adiciones a La Flora Vascular de Los Llanos de Venezuela: Nuevos Registros y Estados Taxonómicos. In *Biollania*; Aymard, G., Ed.; Universidad Nacional Experimental de los Llanos Occidentales "Ezequiel Zamora" UNELLEZ: Guanare, Venezuela, 2017; Vol. 15, pp. 1–296 ISBN 980-231-131-6.
108. Piraquive, D.; Behling, H. Holocene Paleoecology in the Neotropical Savannas of Northern South America (Llanos of the Orinoquia Ecoregion, Colombia and Venezuela): What Do We Know and on What Should We Focus in the Future? *Front. Ecol. Evol.* **2022**, *10*, 824873, doi:10.3389/fevo.2022.824873.
109. Jaramillo, A.; Rangel-Ch, J.O. Los Sistemas Fluviales de La Orinoquía Colombiana. In *Colombia Diversidad Biótica Vol. XIV: La región de la Orinoquia de Colombia*; Rangel-Ch, J.O., Ed.; Universidad Nacional de Colombia, Instituto de Ciencias Naturales: Bogotá, Colombia, 2014; pp. 71–99 ISBN 978-958-775-147-5.
110. Rippstein, G.; Amézquita, E.; Escobar, G.; Grollier, C. Condiciones Naturales de La Sabana. In *Agroecología y diversidad de las sabanas en los Llanos Orientales de Colombia*; Rippstein, G., Escobar, G., Motta, F., Eds.; Centro Internacional de Agricultura Tropical CIAT: Cali, Colombia, 2001; pp. 1–21.
111. IDEAM Zonificación Hidrográfica de Colombia a Escala 1:100.000 Available online: http://www.siac.gov.co/.
112. Farr, T.; Rosen, P.; Caro, E.; Crippen, R.; Duren, R.; Hensley, S.; Kobrick, M.; Paller, M.; Rodriguez, E.; Roth, L.; et al. The Shuttle Radar Topography Mission. *Rev. Geophys.* **2007**, *45*, 1–33, doi:10.1029/2005RG000183.
113. Fick, S.; Hijmans, R. Worldclim 2: New 1-Km Spatial Resolution Climate Surfaces for Global Land Areas. *Int. J. Climatol.* **2017**, *37*, 4302–4315, doi:10.1002/joc.5086.
114. Minorta, V.; Niño, L.; Rangel, O.; Giraldo, D.; Aymard, G.; Sánchez, D. Multicriteria Assessment of Vegetation Threats in the Colombian Orinoquia. *Harvard Pap. Bot.* **2026**, *30*, 29–47, doi:10.3100/hpib.v30iss1.2026.n5.

 doi:10.20944/preprints202604.1593.v1

115. Minorta-Cely, V.; Rangel-Ch, J.O.; Castro, F.; Niño, L.; Aymard, G. Los Bosques de La Orinoquía Colombiana: Composición Florística, Patrones de La Estructura y Sintaxonomía. In *Colombia Diversidad Biótica XXI: Tipos de vegetación en las regiones naturales de Colombia. Nuevos aportes.*; Rangel-Ch, J.O., Ed.; Universidad Nacional de Colombia: Bogotá, Colombia, 2023; pp. 413–587.
116. Minorta-Cely, V.; Rangel-Ch, J.O.; Castro, F.; Niño, L.; Aymard, G. Los Pastizales de La Orinoquia Colombiana: Composición Florística y Sintaxonomía. In *Colombia Diversidad Biótica XXI: Tipos de vegetación en las regiones naturales de Colombia. Nuevos aportes.*; Rangel-Ch, J.O., Ed.; Universidad Nacional de Colombia: Bogotá, Colombia, 2023; pp. 305–412.
117. Franklin, S. Geomorphometric Processing of Digital Elevation Models. *Comput. Geosci.* **1987**, *13*, 603–609.
118. Franklin, S.; Peddle, D. Texture Analysis of Digital Image Data Using Spatial Cooccurrence. *Comput. Geosci.* **1987**, *13*, 293–311.
119. Raed, M.; Gari, J.; Berlles, J.; Sedeño, A.; Porta, P.; Delise, L.; Vicini, E.; Sánchez, L.; Iriondo, J.; Yebrin, J. Métodos de Clasificación Supervisada y No Supervisada de Imágenes SAR ERS 1/2. In Proceedings of the Proceedings of an International Seminar on The Use and Applications of ERS in Latin America; European Space Agency: Viña del Mar, Chile, 1996; pp. 287–292.
120. Fisher, J.; Whittaker, R.; Malhi, Y. ET Come Home: Potential Evapotranspiration in Geographical Ecology. *Glob. Ecol. Biogeogr.* **2011**, *20*, 1–18, doi:10.1111/j.1466-8238.2010.00578.x.
121. O'Brien, E. Water-Energy Dynamics, Climate, and Prediction of Woody Plant Species Richness: An Interim General Model. *J. Biogeogr.* **1998**, *25*, 379–398, doi:10.1046/j.1365-2699.1998.252166.x.
122. Thornthwaite, C. An Approach toward a Rational Classification of Climate. *Geogr. Rev.* **1948**, *38*, 55–94.
123. Hofierka, J.; Súri, M. The Solar Radiation Model for Open Source GIS: Implementation and Applications. In Proceedings of the Proceedings of the Open source GIS - GRASS users conference; Trento. Italy, 2002; pp. 51–70.
124. Mesquita, S.; Sousa, A. Bioclimatic Mapping Using Geostatistical Approaches: Application to Mainland Portugal. *Int. J. Climatol.* **2009**, *29*, 2156–2170, doi:10.1002/joc.1837.
125. Bourbigot, M.; Johnsen, H.; Piantanida, R.; Hajduch, G.; Poullaouec, J. *Sentinel-1 Product Definition*; 2016;
126. Baeza, S.; Paruelo, J.M.; Altesor, A. Caracterización Funcional de La Vegetación Del Uruguay Mediante El Uso de Sensores Remotos. *Interciencia* **2006**, *31*, 382–388.
127. Serbin, S.; Townsend, P. Scaling Functional Traits from Leaves to Canopies. In *Remote Sensing of Plant Biodiversity*; Cavender-Bares, J., Gamon, J., Townsend, P., Eds.; Springer: Cham, Switzerland, 2020; pp. 43–82.
128. Singh, A. Spectral Separability of Tropical Forest Cover Classes. *Int. J. Remote Sens.* **1987**, *8*, 971–979, doi:10.1080/01431168708954741.
129. Sayler, K.; Glynn, T. *Landsat 8-9. Collection 2 (C2). Level 2 Science Product (L2SP) Guide.*; Sioux Falls, South Dakota, 2022;
130. Congalton, R. A Review of Assessing the Accuracy of Classifications of Remotely Sensed Data. *Remote Sens. Environ.* **1991**, 35–46.